MOLECULAR AND CELLULAR BIOLOGY, Jan. 2010, p. 172–185 Vol. 30, No. 1
0270-7306/10/$12.00 doi:10.1128/MCB.00869-09

The Role of Coa2 in Hemylation of Yeast Cox1 Revealed by Its Genetic Interaction with Cox10▽

Megan Bestwick, Oleh Khalimonchuk, Fabien Pierrel,† and Dennis R. Winge*

University of Utah Health Sciences Center, Departments of Medicine and Biochemistry, Salt Lake City, Utah 84132

Received 2 July 2009/Returned for modification 3 August 2009/Accepted 12 October 2009

Saccharomyces cerevisiae **cells lacking the cytochrome *c* oxidase (CcO) assembly factor Coa2 are impaired in Cox1 maturation and exhibit a rapid degradation of newly synthesized Cox1. The respiratory deficiency of *coa2*Δ cells is suppressed either by the presence of a mutant allele of the Cox10 farnesyl transferase involved in heme *a* biosynthesis or through impaired proteolysis by the disruption of the mitochondrial Oma1 protease. Cox10 with an N196K substitution functions as a robust gain-of-function suppressor of the respiratory deficiency of *coa2*Δ cells but lacks suppressor activity for two other CcO assembly mutant strains, the *coa1*Δ and *shy1*Δ mutants. The suppressor activity of N196K mutant Cox10 is dependent on its catalytic function and the presence of Cox15, the second enzyme involved in heme *a* biosynthesis. Varying the substitution at Asn196 reveals a correlation between the suppressor activity and the stabilization of the high-mass homo-oligomeric Cox10 complex. We postulate that the mutant Cox10 complex has enhanced efficiency in the addition of heme *a* to Cox1. Coa2 appears to impart stability to the oligomeric wild-type Cox10 complex involved in Cox1 hemylation.**

Cytochrome *c* oxidase (CcO) is the terminal enzyme of the energy-transducing respiratory chain in mitochondria. Eukaryotic CcO consists of 12 to 13 subunits, with three mitochondrion-encoded subunits (Cox1 to Cox3) forming the core enzyme embedded within the mitochondrial inner membrane (IM). The remaining nucleus-encoded subunits pack on the periphery of the catalytic core (35). The assembled holoenzyme is further organized into supercomplexes with the bc_1 cytochrome *c* reductase (8). The core CcO subunits contain three copper atoms and two modified heme cofactors (34). Cox1 contains both heme moieties, one of which exists as a heterobinuclear center with copper. Cox2 contains the other two Cu ions within a binuclear copper center. Two modifying enzymes, Cox10 and Cox15, form the modified heme moiety in CcO. Cox10 catalyzes the conversion of heme *b* into heme *o* by the addition of a hydroxyethyfarnesyl group (12). Cox15 converts heme *o* into heme *a* through the oxidation of a C_8 pyrrole methyl moiety (11). Cox15, heme *a* synthase, works in conjunction with ferredoxin and ferredoxin reductase (4).

The biogenesis of CcO, occurring within the IM, commences with the mitochondrial synthesis of the Cox1 subunit, followed by stepwise insertion of the heme and copper redox cofactors and the addition of the remaining subunits. The translation of Cox1 on mitoribosomes occurs in juxtaposition to the IM and is mediated in yeast by the IM-tethered translational activators Pet309 and Mss51 (21, 22, 27, 32). Mdm38 and Mba1 facilitate recruitment of mitoribosomes for Cox1 translation (26, 30). Nascent Cox1 appears to be inserted into the IM by the Oxa1 translocase (16). Newly synthesized Cox1 is escorted through the maturation process by IM-associated protein complexes containing Mss51, Cox14, Coa1, and Shy1. The initial Cox1 assembly intermediate involves a complex with Mss51 and Cox14 (3, 27). Cox14 is not important for the translational initiation function of Mss51, since *cox14*Δ cells synthesize Cox1 but are stalled in its maturation presumably due to the failure to form the newly synthesized Cox1-Mss51 complex (3, 27). Coa1 appears to coordinate the transition of newly synthesized Cox1 from the Mss51-Cox14 complex to a later intermediate involving Shy1 that likely functions in the heterobimetallic heme-copper center (23, 28). Cells lacking Coa1 or Shy1 synthesize Cox1, but maturation is largely stalled prior to cofactor insertion, leading to Cox1 degradation. Limited assembly of CcO occurs in either deficient strain, but the residual CcO is insufficient to promote respiratory growth.

Clues to the CcO assembly pathway have been gleaned by the isolation of genetic suppressors of respiration-deficient strains (1). Overexpression of *MSS51* in *shy1*Δ cells yields respiratory growth, most likely through elevated Cox1 translation (2). Mss51 was proposed to be sequestered in a nonproductive complex in *shy1*Δ cells, thereby limiting its level for Cox1 translation initiation (3). Overexpression of Hap4, the catalytic subunit of the Hap2/3/4/5 transcription complex, suppresses the CcO deficiency of *shy1*Δ cells through induced expression of nucleus-encoded subunits of CcO (10). Enhanced levels of Cox5a and Cox6 may stabilize Cox1 in *shy1*Δ cells, enabling progression to later stages of CcO assembly. A series of extragenic suppressors of the *coa1*Δ cell respiratory defect was isolated (28). High-copy-number *MSS51* was an efficient suppressor of *coa1*Δ cells, and three weaker suppressors were high-copy-number *COX10*, *MDJ1*, and *COA2*. As described, Cox10 is involved in the biosynthesis of heme *a*, Mdj1 is a DnaJ cochaperone with Hsp70, and Coa2 is a newly identified CcO assembly factor. Strong synergism was observed

* Corresponding author. Mailing address: University of Utah Health Sciences Center, Departments of Medicine and Biochemistry, Salt Lake City, UT 84132. Phone: (801) 585-5103. Fax: (801) 585-3432. E-mail: dennis.winge@hsc.utah.edu.

† Present address: Laboratoire de Chimie et de Biologie des Métaux, CEA, Grenoble, France.

▽ Published ahead of print on 19 October 2009.

TABLE 1. *S. cerevisiae* yeast strains used in this study

Strain	Genotype	Source or reference(s)
BY4741	*MAT***a** *his3Δ1 leu2Δ0 met15Δ0 ura3Δ0*	Invitrogen
BY4741 *coa2*Δ	*MAT***a** *his3Δ1 leu2Δ0 met15Δ0 ura3Δ0 coa2*::*kanMX4*	29
BY4743	*MAT***a**/α *his3Δ1/his3Δ1 leu2Δ0/leu2Δ0 LYS2/lys2Δ0 MET15/met15Δ0 ura3Δ0/ura3Δ0*	Invitrogen
BY4743 *cox10*Δ	BY4743 *cox10*::*kanMX4*	Invitrogen
BY4743 *coa1*Δ	BY4743 *coa1*::*kanMX4*	Invitrogen
BY4743 *shy1*Δ	BY4743 *shy1*::*kanMX4*	Invitrogen
W303	*MAT*α *ade2-1 his3-1,15 leu2-3,112 trp1-1*, *ura3-1*	
W303 *coa2*Δ	W303 *coa2*::*kanMX4*	29
W303 *cox10*Δ	W303 *cox10*::*HIS3*	25
W303 *coa1*Δ	W303 *coa1*::*kanMX4*	23, 28
W303 *cox4*Δ	W303 *cox4*::*CaURA3*	13
W303 *cox11*Δ	W303 *cox11*::*HIS3*	7
W303 *oma1*Δ	W303 *oma1*::*CaURA3*	This work
W303 *coa2*Δ*yta12*Δ	W303 *coa2*::*CaURA3 yta12*::*kanMX4*	29
W303 *coa2*Δ*yme1*Δ	W303 *coa2*::*CaURA3 yme1*::*kanMX4*	This work
W303 *coa2*Δ*oma1*Δ	W303 *coa2*::*kanMX4 oma1*::*CaURA3*	This work
W303 *coa2*Δ*cox15*Δ	W303 *coa2*:: *kanMX4 cox15*::*CaURA3*	This work
DY5113 (W303)	*MAT***a** *ade2-1 his3-1,15 leu2-3,112 trp1*Δ, *ura3-1*	
COX10-3HA	DY5113 *COX10*-3HA::*TRP1*	This work
COX10-13Myc	DY5113 *COX10*-13Myc::*TRP1*	This work
COX10-13Myc *mss51*Δ	DY5113 *COX10*-13Myc::*TRP1 mss51*::*kanMX4*	This work
COX10-13Myc *cox14*Δ	DY5113 *COX10*-13Myc::*TRP1 cox14*::*CaURA3*	This work
COX10-13Myc *coa1*Δ	DY5113, *COX10*-13Myc::*TRP1*, *coa1*::*CaURA3*	This work
COX10-13Myc *shy1*Δ	DY5113 *COX10*-13Myc::*TRP1 shy1*::*CaURA3*	This work
COX10-13Myc *sco1*Δ	DY5113 *COX10*-13Myc::*TRP1 sco1*::*kanMX4*	This work
COX10-13Myc *cox1*Δ	*MAT*α *lys2 leu2-3,112 arg8*::*hisG ura3-52 cox1*Δ::*ARG8m COX10*-13Myc::*kanMX*	This work
COX15-13Myc	DY5113 *COX15*-13Myc::*TRP1*	This work
SHY1-13Myc	DY5113 *SHY1*-13Myc::*TRP1*	29
SHY1-13Myc *cox11*Δ	DY5113 *SHY1*-13Myc::*TRP1 cox11*::*HIS3*	This work
COA1-13Myc	DY5113 *COA1*-13Myc::*HIS3*	23, 28
COX1-3HA	*MAT***a** *arg8*::*hisG leu2-3,112 lys2 ura3-52 COX1*-3HA D273-10B	X. Perez-Martinez

with *MSS51* in combination with either *COX10* or *COA2* in the suppression of both *coa1*Δ and *shy1*Δ cells (29).

Coa2 is a small matrix-localized protein that functions downstream of the Mss51-dependent step in Cox1 maturation (29). The observed transient interaction of Coa2 and Shy1 suggested a role in the ShyI-related step in Cox1 maturation. One dramatic phenotype of *coa2*Δ cells is the rapid degradation of newly synthesized Cox1 (29). High-copy-number Mss51, which efficiently suppresses the respiratory defect of *coa1*Δ and *shy1*Δ cells, had no effect in *coa2*Δ cells, although high-copy-number Cox10 was weakly effective. During these studies, we observed spontaneous mutant clones of *coa2*Δ cells with robust respiratory growth. In the present study we report the characterization of a mutant allele of *COX10* that is a dominant suppressor of *coa2*Δ cells. We show that the suppressor activity of mutant Cox10 is dependent on its catalytic activity and suggest that the mutant Cox10 facilitates heme *a* addition into Cox1, a step that is compromised in *coa2*Δ cells. Coa2 per se is not essential for hemylation of Cox1, since CcO biosynthesis can be restored in *coa2*Δ cells by depleting cells of the metallopeptidase Oma1. The present work provides novel insight into the function of Cox10, Coa2, and Oma1.

MATERIALS AND METHODS

Yeast strains and vectors. The *Saccharomyces cerevisiae* yeast strains used in this study are listed in Table 1. The hemagglutinin (HA)-tagged Cox1 strain was a generous gift from Xochitl Perez-Martinez. Strains with open reading frame (ORF) deletions generated for this work were created by homologous recombination of disruption cassettes using either *KanMX4* or *Candida albicans URA3*. Strains with an integrated 3′-13Myc or 3′-3HA epitope tag were generated as described previously (20). All strains generated for this work were confirmed by PCR. The *COX10* ORF was cloned into plasmid pRS426 and pRS416 under the control of its own promoter and terminator (450 base pairs upstream and downstream of the ORF). The N196K mutation was made in both the high- and low-copy-number vectors using site-directed mutagenesis. The *COX10* ORF with a 3′-13Myc tag was cloned from genomic DNA of the DY5113 *COX10*-13Myc strain into pRS416 and pRS415 vectors under the control of its own promoter and the *ADH1* terminator. The N196K, N196A, N196D, R212,216A, and H317A mutations were generated by site-directed mutagenesis. Successive rounds of site-directed mutagenesis created the double and triple mutations. The *COX15* ORF with a 3′-6His epitope tag was cloned into pRS423 under the control of the *MET25* promoter and *CYC1* terminator. The *YAH1* ORF was cloned into pRS425 under the control of its own promoter (450 base pairs upstream of the ORF) and the *CYC1* terminator. Sequencing was used to confirm all cloning and site-directed mutagenesis products in the vectors created. The *MSS51*, *COA2*, and *YTA12* (E614Q) vectors used have been previously described (29). Yeast strains were transformed using lithium acetate. Culture conditions for the yeast strains were either rich medium (YP) or synthetic complete (SC) medium lacking the appropriate nutrients for plasmid selection.

Mitochondrial purification and assays. Intact mitochondria were isolated from yeast as previously described (9). The standard Bradford assay was used to determine total mitochondrial protein concentration (5). Total heme was extracted from 1 to 2 mg of purified mitochondria with 0.5 ml acetone containing 2.5% HCl as described previously (4). The pH of the extract was adjusted to 4.0 by the addition of 1 μl formic acid and titration with 5 M KOH (elution times are affected by the pH). The sample was clarified by centrifugation at 13,000 rpm for 5 min, and 1 ml was injected onto a 4.6- by 250-mm SunFire C_{18} 5-μm column (Waters). Hemes were eluted from the column at a flow rate of 1 ml/min using a 30 to 50% gradient of acetonitrile containing 0.05% trifluoroacetic acid for the first 3 ml and a 50 to 80% gradient for the next 42 ml. The elution of heme compounds was monitored at 400 nm; purified heme *a*, heme *o*, and hemin were used as standards to determine elution times. Heme *a* was a generous gift from Winslow Caughey.

Blue native PAGE. Blue native PAGE (BN-PAGE) was performed essentially as described previously (38) with 1% digitonin. After incubation on ice for 15 min and centrifugation (20,000 × *g* for 15 min at 2°C), supernatants were mixed with sample buffer (5% Coomassie brilliant blue G250, 0.5 M 6-aminocaproic acid, pH 7.0) and then loaded on a gradient polyacrylamide gel. Separated complexes were detected by immunoblotting on a polyvinylidene difluoride (PVDF) membrane. The high-mass marker proteins were obtained from GE Healthcare.

Immunoblotting. Mitochondrial protein samples were separated on 12% polyacrylamide gels and transferred to nitrocellulose. Proteins were visualized using either enhanced chemiluminescence (ECL) reagents with horseradish peroxidase-conjugated secondary antibodies or the Odyssey infrared imaging system (Li-Cor Biosciences) with fluorescent secondary antibodies (anti-mouse IRDye 800 and anti-rabbit IRDye 680; Li-Cor Biosciences). Anti-Myc and anti-HA rabbit polyclonal antisera was purchased from Santa Cruz, anti-Myc and anti-HA mouse monoclonal antibodies were from Roche, antiporin was from Molecular Probes, and anti-Cox2 was from Mitosciences. Alex Tzagoloff generously provided antiserum to F_1 ATP synthase, and Thomas Langer provided antisera to Phb1 and Phb2.

IP. Immunoprecipitations (IPs) were performed essentially as described previously (29) except that the IP buffer used was 20 mM Tris (pH 7.4), 50 mM sodium chloride, 1 mM phenylmethylsulfonyl fluoride, and 1% digitonin. Anti-HA–agarose and anti-Myc–agarose conjugates were purchased from Santa Cruz. The clarified lysate, unbound, final wash, and elution fractions were analyzed by immunoblotting.

Additional assays. The respiratory competency of strains was determined by growth tests on plates containing 2% glucose or 2% glycerol–2% lactate as a carbon source. Yeast cells were grown overnight in liquid cultures in selective medium containing 2% raffinose–0.2% glucose and adjusted to an optical density at 600 nm (OD_{600}) of 0.5, and serial dilutions were spotted onto the plates and incubated at 30°C for 2 days (glucose plates) or 4 to 6 days (glycerol-lactate plates). The oxygen consumption of cells grown to stationary phase was determined on a 5300A biological oxygen monitor (Yellow Springs Instrument Co.). The rate of oxygen consumption (% O_2/second/OD_{600} unit) was calculated from the linear response (17). For *in vivo* mitochondrial labeling with [^{35}S]methionine, cells were grown overnight in selective medium containing 2% raffinose–0.2% glucose and then reinoculated into YP–2% galactose to grow to an OD_{600} of 1. The labeling and preparation of the samples for 12% SDS-PAGE have been described previously (2). Gels were dried, and radiolabeled proteins were visualized by exposing autoradiographic films at −80°C. Sensitivity of yeast strains to hydrogen peroxide was determined as previously described (19).

Construction of the low-copy-number library. Genomic DNA purified from the *coa2*Δ suppressor strain containing the *COX10*-N196K mutation was partially digested with Sau3A. DNA fragments were then purified from an agarose gel and ligated with plasmid pRS416 that was digested to completion with BamHI. The resulting number of transformants was sufficient for severalfold coverage of the yeast genome.

RESULTS

Isolation of a *coa2*Δ dominant suppressor. Coa2 is required for the assembly of CcO in yeast (29). Cells lacking Coa2 fail to propagate on glycerol/lactate growth medium (29) (Fig. 1A). With prolonged incubation on glycerol/lactate medium, spontaneous mutants emerged that showed robust growth upon subsequent replating. The frequencies of appearance of spontaneous mutants were 1 in 10^7 colonies for *coa2*Δ cells in the BY4741 background and 1.7 in 10^6 colonies for *coa2*Δ cells in the W303 background. Recovery of one spontaneous suppressor clone showed that upon subsequent plating, respiratory growth resembled that of wild-type (WT) cells (Fig. 1A). *coa2*Δ null cells exhibit a marked attenuation of newly synthesized Cox1 in an *in vivo* translation assay, and this attenuation was shown to arise from enhanced degradation rather than impaired translation (29). The suppressor mutant showed normal Cox1 levels in the *in vivo* translation assay (Fig. 1B). To assess whether the suppressing mutation was recessive or dominant, the suppressor isolate was crossed with the parent *coa2*Δ strain of opposite mating type. The resulting diploid strain was found to be respiration competent in showing WT growth on glycerol/lactate medium. The diploid was sporulated, and tetrad dissection revealed that the suppressing phenotype segregated 2:2, suggesting that a single mutant gene was responsible for the phenotype.

To clone the dominant mutant gene, a genomic library was constructed from the genomic DNA of the suppressor *coa2*Δ clone in a centromeric vector. Recombinant plasmid DNA was used to transform *coa2*Δ parent cells, and transformants that grew on glycerol/lactate medium were isolated. The respiratory growth was shown to be dependent on the library vector, as shedding the vector by growth in 5-fluorortate abrogated respiratory growth. The plasmid rescued from the respiration-competent *coa2*Δ cells was used to retransform *coa2*Δ cells, and respiratory competence was recovered. DNA sequencing revealed the suppressor gene to be a mutated *COX10* causing an N196K amino acid change. Asn196 is a highly conserved residue in diverse Cox10 orthologs (Fig. 1C).

The N196K mutation was introduced in a low-copy-number plasmid containing *COX10* and transformed into *coa2*Δ or *cox10*Δ cells (Fig. 1D). The mutant Cox10 restored respiratory growth in *coa2*Δ cells, demonstrating that the mutation was sufficient to confer the suppressor phenotype. WT *COX10* is only a weak suppressor in *coa2*Δ cells when expressed in high copy number, a situation similar to its weak suppressor activity in *coa1*Δ cells (28, 29). The observed respiratory growth of *cox10*Δ cells harboring the N196K mutant allele showed that the substitution did not impair the catalytic activity of Cox10. This conclusion was substantiated by the observation that oxygen consumption by *cox10*Δ cells containing either WT Cox10 or the N196K mutant protein was similar (Fig. 1E). No dominant negative effects were observed in transformants of WT cells with the mutant Cox10 regardless of whether it was expressed from a low- or high-copy-number vector.

The presence of the mutant Cox10 in *coa2*Δ cells restored Cox1 levels in the *in vivo* mitochondrial translation assay (Fig. 1F) better than the WT Cox10 protein. Likewise, mutant Cox10 restored Cox1 levels in *cox10*Δ cells.

N196K Cox10 is a *coa2*Δ-specific suppressor. N196K Cox10 has a gain-of-function activity in *coa2*Δ cells. To substantiate this activity, we engineered the mutation in a *cox10* allele encoding a double substitution of two functionally important conserved Arg residues implicated in the binding of the pyrophosphate moiety of the farnesyl pyrophosphate substrate of the Cox10-related CyoE heme *o* synthase of *Escherichia coli* (31). The double-Arg Cox10 mutant (R212,216A) was nonfunctional in *cox10*Δ cells (Fig. 1D) and failed to suppress either *coa1*Δ cells (28) or *coa2*Δ cells despite the presence of the mutant protein by immunoblotting (data not shown). However, the triple mutant (N196K, R212,216A) retained the suppressor activity in *coa2*Δ cells and, surprisingly, restored Cox10 function in *cox10*Δ cells (Fig. 1D and E). Thus, the N196K substitution has a dominant effect on the Cox10 suppressor activity.

We previously demonstrated that high-copy-number *COX10* was a weak suppressor of *coa1*Δ and *shy1*Δ cells (28). To assess whether the N196K mutant Cox10 exhibited gain-of-function suppressor activity in these cells, low- and high-copy-number vectors carrying either WT or mutant *COX10* were transformed in *coa1*Δ and *shy1*Δ cells, and respiratory growth was

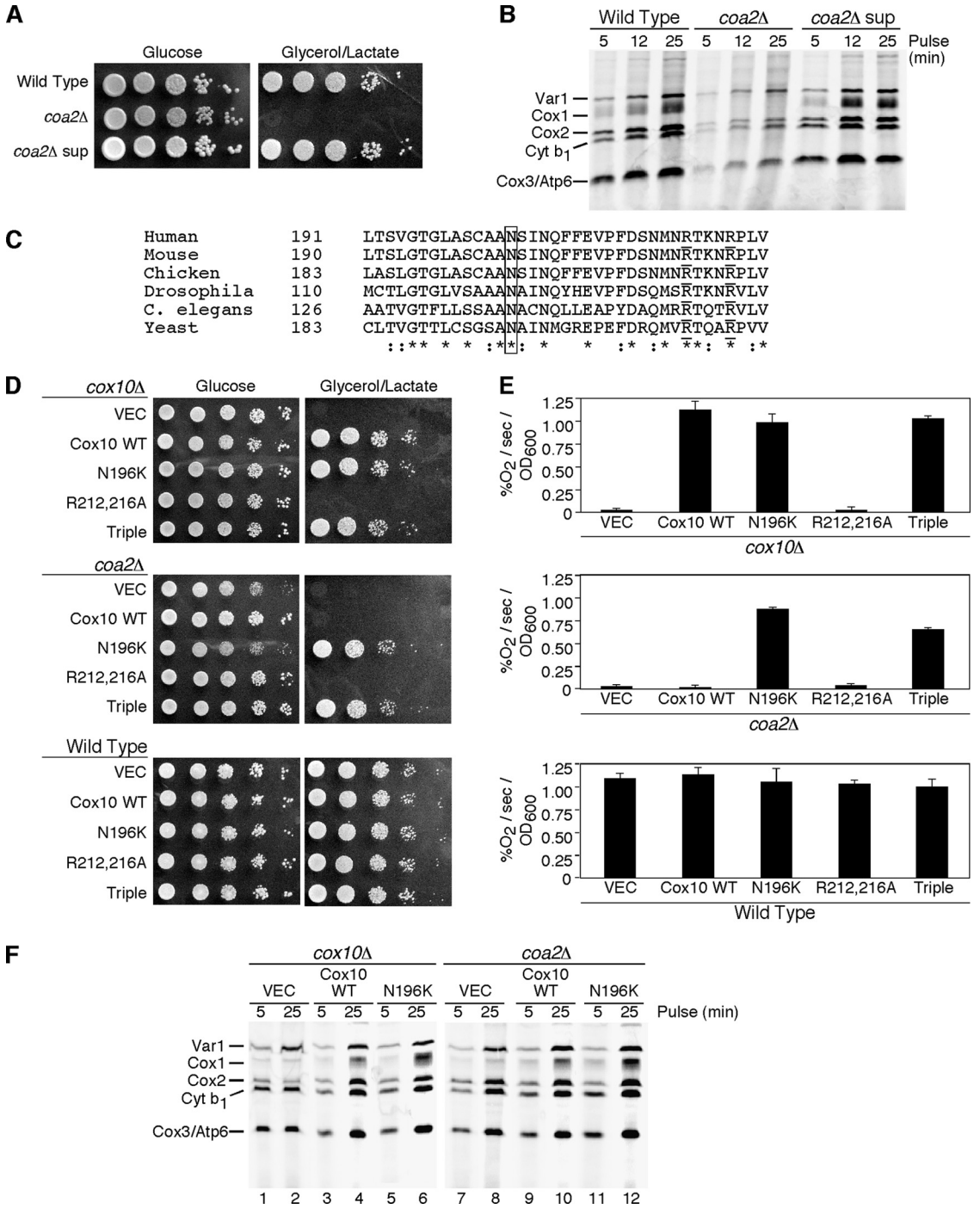

FIG. 1. Identification of the *coa2*Δ suppressor mutant as N196K Cox10. (A) W303 wild type (WT), *coa2*Δ, and isolated *coa2*Δ suppressor strains were grown in yeast extract-peptone-dextrose, serially diluted, and spotted on yeast extract–peptone–2% glucose and yeast extract–peptone–2% glycerol-2% lactate. Plates were grown at 30°C. (B) *In vivo* labeling of mitochondrial translation products. The strains described for panel A were pulsed with [^{35}S]methionine for 5, 12, and 25 min at 30°C. The samples were separated by 12% SDS-PAGE, and the gel was dried and then exposed to autoradiographic film. (C) Alignment of the peptide sequences of Cox10 from various species using ClustalW. The box highlights the conserved N196 residue. Arg212 and Arg216, residues required for activity, are underlined. Residues with conserved substitutions across species are indicated by colons, and identical residues across species are indicated by asterisks. (D) BY *cox10*Δ, *coa2*Δ, and wild-type cells transformed with centromeric vectors expressing WT Cox10, N196K Cox10, R212A,R216A Cox10, and N196K,R212A,R216A Cox10 (Triple) were grown in SC–2% raffinose–0.2% glucose selective medium, serially diluted, and spotted on SC–2% glucose and SC–2% glycerol–2% lactate. The plates were incubated at 30°C. Similar results were observed for cells transformed with episomal vectors. (E) The cells described for panel D were grown in liquid SC–1% glucose overnight, and oxygen consumption (% O_2/second/OD_{600} unit) was measured. The data represent the averages of four independent repeats, and the error bars represent standard errors of the means. (F) *In vivo* labeling of mitochondrial translation products. W303 *cox10*Δ cells (lanes 1 to 6) and W303 *coa2*Δ cells (lanes 7 to 12) transformed with episomal vectors expressing WT Cox10 and N196K Cox10 were pulsed with [^{35}S]methionine for 5 and 25 min. The samples were analyzed as described for panel B.

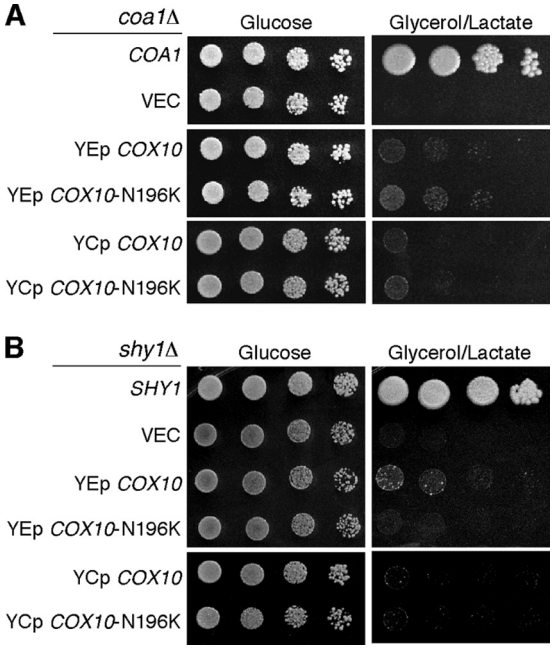

FIG. 2. N196K Cox10 does not alter suppression of the respiratory defect of *coa1*Δ or *shy1*Δ cells. (A) BY *coa1*Δ cells transformed with either episomal (YEp) or centromeric (YCp) vectors expressing WT *COX10* or *COX10* (N196K) were grown in SC–2% raffinose–0.2% glucose selective medium, serially diluted, and spotted on SC–2% glucose and SC–2% glycerol–2% lactate agar plates. The plates were incubated at 30°C. (B) BY *shy1*Δ cells with either YEp or YCp vectors expressing WT *COX10* or *COX10* (N196K) were treated as described for panel A.

assessed (Fig. 2). The WT and mutant genes were equally weak suppressors in these CcO assembly mutants. In addition, no suppression by the N196K Cox10 was seen in *cox14*Δ cells (data not shown). Thus, the N196K Cox10 has a unique suppressor function in *coa2*Δ cells.

The N196K mutant Cox10 may exert its specific suppressor function in *coa2*Δ cells by one of two mechanisms. The first scenario is that the mutant Cox10 has a gain-of-function role in directly stabilizing newly synthesized Cox1, thereby impairing proteolytic degradation. The second candidate mechanism is that mutant Cox10 has an enhanced efficiency in heme *a* site formation in Cox1. The marked instability of Cox1 seen in *coa2*Δ cells may arise from an impaired addition of heme *a*, since the heme *a* site stabilizes the Cox1 helical bundle. Studies were conducted to discern between these candidate mechanisms of suppression.

N196K Cox10 has no general role in the stabilization of Cox1. The first postulate is that the N196K mutant Cox10 has a gain-of-function role in stabilizing Cox1 within early assembly intermediates. One marked phenotype of *coa2*Δ cells is the rapid degradation of Cox1 observed with *in vivo* mitochondrial translation assays (29) (Fig. 1F). We conducted three studies to test this first postulate. First, Coa1 and Shy1 participate in early Cox1 assembly intermediates downstream of the Mss51-Cox14 complex and have previously been shown to bind Cox1 (23, 28). To assess whether N196K mutant Cox10 had an effect on the abundance of these Cox1 assembly complexes, mitochondria isolated from cells chromosomally epitope tagged at the *COA1* and *SHY1* loci were fractionated on BN-PAGE (Fig. 3A). The presence of N196K Cox10 had no effect on the abundance of Cox1-containing high-mass Coa1 and Shy1 complexes. The high-mass Shy1 complex is attenuated in numerous CcO assembly mutants, such as *cox11*Δ cells (Fig. 3A, lane 8). The N196K mutant Cox10 had no stabilizing effect on the Cox1-containing ~450-kDa Shy1 complex in these cells (Fig. 3, lane 9). Second, the N196K mutant Cox10 fails to stabilize Cox1 in two CcO assembly mutants (*coa1*Δ and *cox4*Δ cells) in which newly synthesized Cox1 is proteolytically unstable (Fig. 3B). Cox1 is synthesized in *coa1*Δ and *cox4*Δ cells as seen in an *in vivo* mitochondrial translation assay, but it is degraded during the chase phase of the assay. The presence of either WT Cox10 or the N196K mutant failed to retard Cox1 degradation in either mutant strain. Third, mutant Cox10 lacks any Cox1 stabilization function as determined using a hydrogen peroxide sensitivity assay. Cells lacking Cox11 are sensitive to hydrogen peroxide due to the accumulation of a stalled heme a_3-Cox1 assembly intermediate (19). We reported previously that overexpression of either *COX10* or *COA2* exacerbated the sensitivity of *cox11*Δ cells to peroxide, most likely through stabilizing the heme a_3-Cox1 assembly intermediate (29). The N196K mutant Cox10 did not induce any further peroxide hypersensitivity to *cox11*Δ cells relative to WT Cox10 (Fig. 3C). These three studies argue against mutant Cox10 having any general Cox1 stabilization function and further support the specific suppression of *coa2*Δ cells.

Suppressor activity of N196K Cox10 is dependent on its catalytic activity. The second candidate mechanism of suppression by the N196K mutant Cox10 is related to its role in heme *a* biosynthesis. Suppression of *coa2*Δ cells by the mutant Cox10 may arise from more efficient hemylation of Cox1. If Coa2 functions at a point in which the heme *a* site is formed, the absence of Coa2 may destabilize the heme *a* site occupancy, leading to an altered Cox1 conformation that is susceptible to proteolytic degradation. To test whether N196K Cox10 had enhanced catalytic activity, we evaluated whether strains harboring the mutant had elevated levels of heme *o* (Fig. 4A). The mutant and WT Cox10 proteins were expressed in either *cox10*Δ or *coa2*Δ cells. Mitochondria purified from each transformant were quantified for various hemes using reverse-phase high-pressure liquid chromatography (HPLC) after organic extraction (Fig. 4A, inset). Comparable levels of heme *a* were evident in *cox10*Δ cells containing either the WT or the N196K Cox10 mutant (80 and 85% of WT level, respectively), but no heme *o* was evident in either extraction. The detection limit for heme *o* in our assay is 10% of heme *a* levels. Likewise, *coa2*Δ cells harboring either the WT or the N196K Cox10 mutant had no detectable levels of heme *o*.

His317 of Cox10 is a highly conserved residue and is implicated in catalytic activity (24). To test whether the suppressor activity of the N196K Cox10 mutant was dependent on the catalytic activity of the enzyme, an H317A substitution was engineered in WT and N196K Cox10 and the resulting mutants were tested for function in *cox10*Δ cells or suppressor activity in *coa2*Δ cells (Fig. 4B). The H317A Cox10 mutant failed to support respiratory growth when expressed in *cox10*Δ cells, as was true with the double H317A,N196K mutant. Immunoblotting revealed that the single H317A mutant was unstable when expressed in *cox10*Δ cells, but the double H317A,N196K mu-

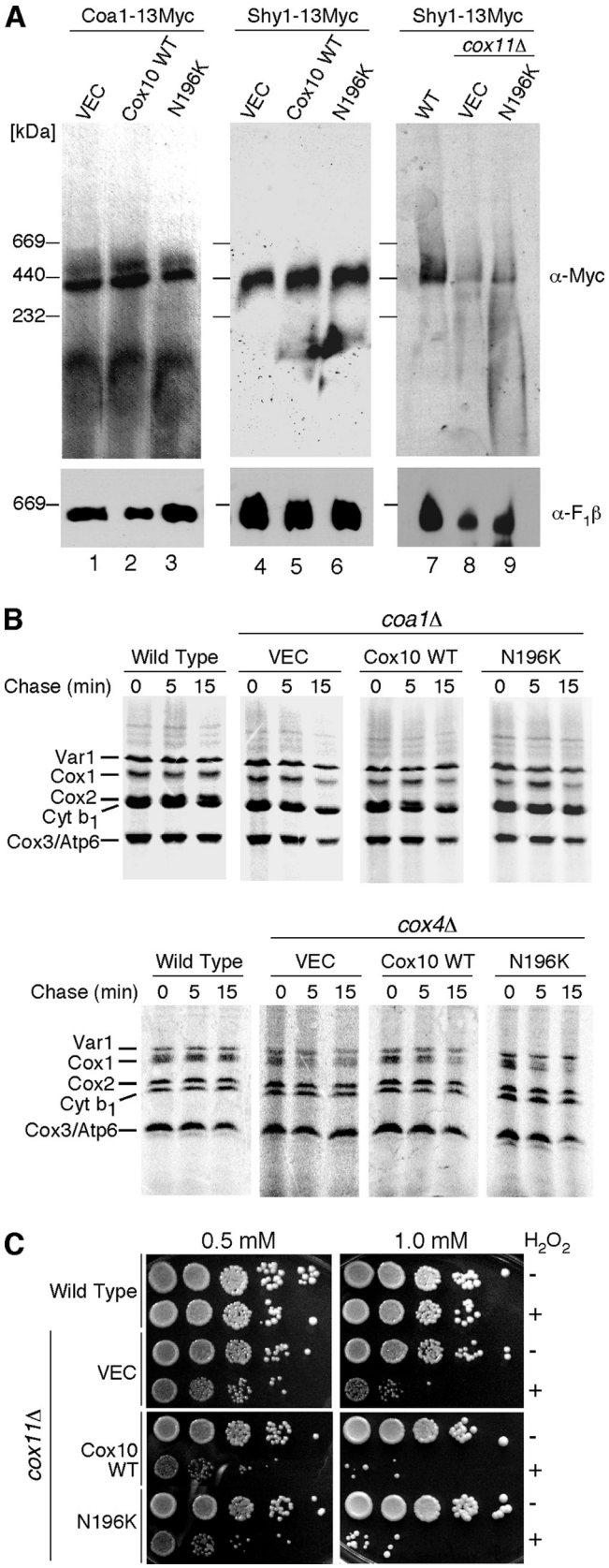

FIG. 3. Stabilization of Cox1 by N196K Cox10 is specific to *coa2*Δ cells. (A) Mitochondria (50 μg protein) isolated from strains containing a genomically tagged 13-Myc *COA1* gene (lanes 1 to 3) or *SHY1* gene (lanes 4 to 6) and expressing either WT Cox10 or N196K Cox10 were solubilized in buffer containing 1% digitonin. Lysates were loaded onto a continuous 5 to 13% gradient gel, and protein complexes were separated by BN-PAGE. Complexes were analyzed by immunoblotting with anti-Myc antibody. Molecular mass markers are indicated, and antibody to the $F_1\beta$ subunit of monomeric complex V was used as a loading control. Mitochondria (50 μg protein) isolated from WT, *cox11*Δ, or *cox11*Δ cells expressing N196K Cox10 and containing an endogenously tagged *SHY1*-13Myc (lanes 7 to 9) were solubilized, separated by BN-PAGE, and analyzed by immunoblotting as in the first two panels. (B) *In vivo* labeling of mitochondrial translation products. W303 WT, *coa1*Δ, and *cox4*Δ cells transformed with WT Cox10 or N196K Cox10 were used in the translation assay as described for Fig. 1B. (C) *cox11*Δ cells transformed with YCp Cox10 or YCp N196K Cox10 vectors and W303 WT cells were grown to mid-exponential phase and incubated with (+) or without (−) the indicated concentrations of H_2O_2 for 2 h at 30°C. Serial dilutions were spotted onto yeast extract-peptone-dextrose plates and incubated for 36 to 48 h at 30°C. Similar results were obtained for YEp *COX10* and N196K *COX10* in the *cox11*Δ background.

tant was stably expressed (Fig. 4C). In addition to the respiratory deficiency of *cox10*Δ transformants with the double H317A,N196K mutant, steady-state levels of Cox2 were also attenuated as seen in the parent *cox10*Δ cells (Fig. 4C). Expression of the mutants in *coa2*Δ cells revealed that the H317A,N196K double mutant failed to suppress the respiratory deficiency of *coa2*Δ cells. Whereas expression of the N196K mutant Cox10 in *coa2*Δ cells resulted in stable Cox1 levels seen in the mitochondrial translation assay, expression of the H317A,N196K double mutant showed a rapid degradation of Cox1 similar to that seen in untransformed *coa2*Δ cells (Fig. 4D). To corroborate the evidence that heme *a* biosynthesis was essential for the suppressor activity of the N196K mutant Cox10, we tested whether the N196K mutant Cox10 retained suppressor activity in stabilizing Cox1 in the mitochondrial translation assay in cells lacking Cox15, the second enzyme required in heme *a* biosynthesis. The N196K mutant Cox10 was expressed in *coa2*Δ *cox15*Δ cells (Fig. 4E). In the mitochondrial translation assay, no Cox1 was observed during the pulse despite the presence of the N196K Cox10. Thus, the catalytic activity of Cox10 and the synthesis of heme *a* are essential for the suppression of respiratory function and Cox1 stabilization in *coa2*Δ cells.

We addressed the specificity of the Asn196 substitution for the gain-of-function suppressor activity in *coa2*Δ cells. Two mutations were introduced into *COX10*, yielding N196A and N196D substitutions, and these mutants were expressed in *cox10*Δ or *coa2*Δ cells (Fig. 4B). None of the substitutions at Asn196 altered the function of Cox10, since all *cox10*Δ transformants grew well on glycerol/lactate medium. However, the N196D mutant Cox10 lacked suppressor activity in *coa2*Δ cells, and the N196A Cox10 yielded only partial restoration of respiratory growth. Thus, the charge at position 196 appears to be important for suppressor activity. The glycerol/lactate growth results matched the stabilization of Cox1 in the mitochondrial translation assay (Fig. 4D).

Suppressor activity of N196K Cox10 correlates with the abundance of its high-mass complex. The N196K Cox10 was reproducibly more abundant relative to the WT protein when expressed in *cox10*Δ and *coa2*Δ cells (Fig. 4C) or WT cells

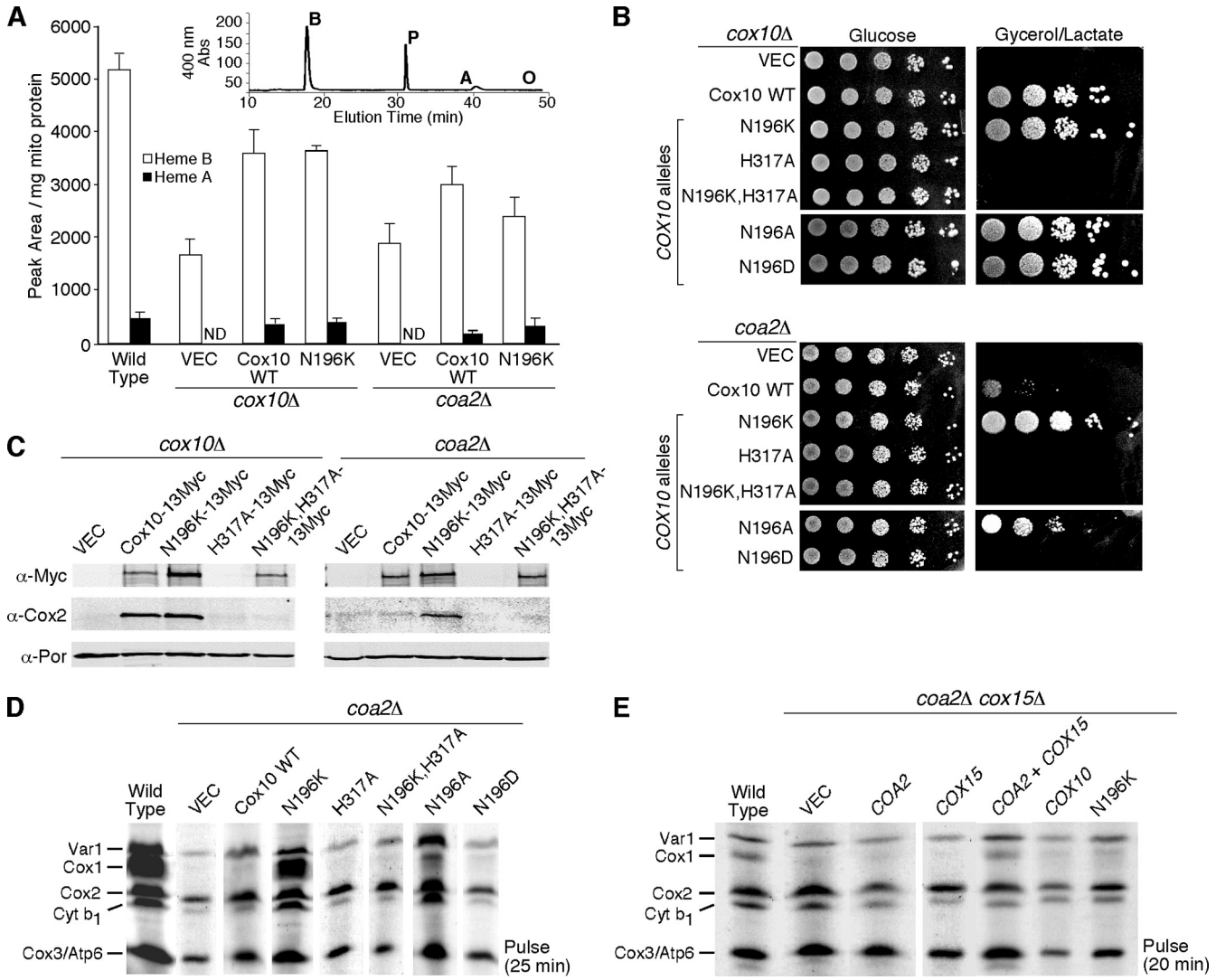

FIG. 4. Catalytically active Cox10 and heme *a* generation are required for suppressor activity by N196K Cox10. (A) Heme was extracted from mitochondria (1.5 to 2 mg protein) isolated from WT cells, *cox10*Δ cells expressing YCp WT Cox10 or N196K Cox10, and *coa2*Δ cells expressing YCp WT Cox10 or Cox10-N196K and separated by reverse-phase high-performance liquid chromatography. The inset shows a representative chromatogram from WT mitochondria. The peaks corresponding to heme *b* (B), heme *a* (A), and protoporphyrin (P) and the expected elution time of heme *o* (O) are indicated. The white bars indicate the area under the heme *b* peak normalized to mg of mitochondrial protein, and the black bars represent the area under the heme *a* peak also normalized to mg of mitochondrial protein. The data represents the averages of three independent repeats, and the error bars represent the standard errors of the means. ND, not detectable. (B) *cox10*Δ and *coa2*Δ cells expressing WT Cox10, N196K Cox10, H317A Cox10, N196K-H317A Cox10, N196A Cox10, and N196D Cox10 were grown in SC–2% raffinose–0.2% glucose selective medium, serially diluted, and drop tested on SC–2% glucose or yeast extract–peptone–2% glycerol-2% lactate. The plates were incubated at 30°C for 2 days (glucose) or 4 days (glycerol/lactate). (C) Purified mitochondria (30 μg protein) from *cox10*Δ and *coa2*Δ cells expressing WT Cox10-13Myc, N196K Cox10-13Myc, H317A Cox10-13Myc, and N196K-H317A Cox10-13Myc were separated by SDS-PAGE and analyzed by immunoblotting using anti-Myc, anti-Cox2, and anti-Por1 (loading control) antibodies. (D) *In vivo* mitochondrial translation. W303 *coa2*Δ cells expressing WT Cox10, N196K Cox10, H317A Cox10, N196K-H317A Cox10, N196A Cox10, and N196D Cox10 were pulsed with [^{35}S]methionine as for Fig. 1B. (E) Analysis of mitochondrial translation products in W303 *coa2*Δ *cox15*Δ cells expressing *COA2*, *COX15*, WT *COX10*, and *COX10* (N196K). The cells were pulsed with [^{35}S]methionine for 20 min at 30°C and analyzed as for Fig. 1B.

(data not shown). To gain further insights into Cox10 function, we carried out BN-PAGE on Myc-tagged Cox10 (Fig. 5A). Cox10 forms a high-mass complex when expressed either from a vector or chromosomally (Fig. 5A, lanes 2 and 7). Surprisingly, the N196K mutant protein forms a markedly more abundant high-mass complex than the WT protein (Fig. 5A, lanes 3 and 6). The presence of the untagged N196K mutant Cox10 in WT cells containing a chromosomally tagged *COX10* also yields a marked enhancement in the abundance of the high-mass complex (Fig. 5A, lanes 8 and 9). Importantly, the high-mass Cox10 complex is gone in *coa2*Δ cells (Fig. 5A, lane 5) despite the presence of the protein seen by SDS-PAGE (Fig. 4C). The N196K mutant protein forms an abundant complex in *coa2*Δ cells (Fig. 5A, lane 6). BN analyses were carried out on mutant Cox10 alleles with various Asn196 substitutions. The N196D mutant, which lacked suppressor activity (Fig. 4B), also

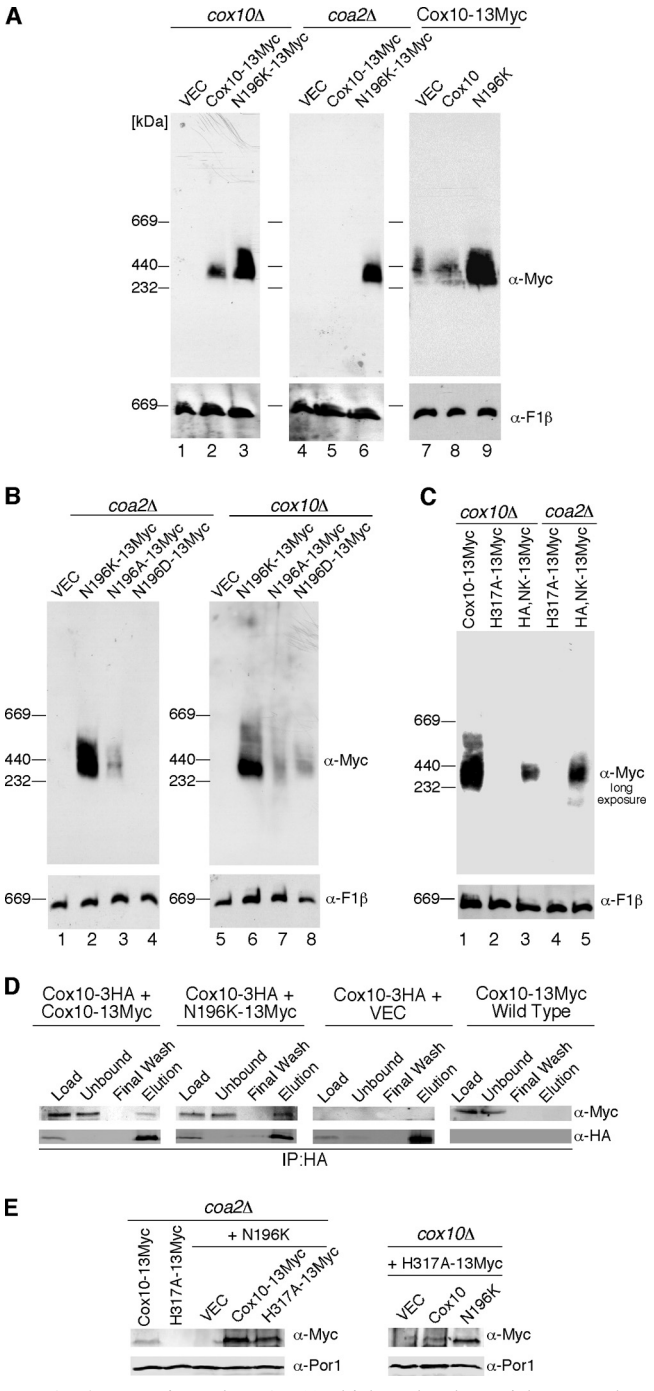

FIG. 5. Assessing the Cox10 high-molecular-weight complex. (A) Purified mitochondria (100 μg protein) from *cox10*Δ and *coa2*Δ cells expressing WT Cox10-13Myc and N196K Cox10-13Myc (lanes 1 to 6) were solubilized in buffer containing 1% digitonin. Lysates were loaded onto a 5 to 13% gradient gel, and complexes were separated by BN-PAGE. Lanes 7 to 9 show the BN-PAGE analysis of mitochondria (100 μg protein) isolated from a genomically tagged *COX10*-13Myc strain expressing WT Cox10 or N196K Cox10 (both untagged). The Cox10-13Myc complex was detected by immunoblotting using anti-Myc antibody in all panels, and monomeric complex V was detected using anti-F1β antibody as a loading control. (B) Purified mitochondria (100 μg proteins) from both *coa2*Δ and *cox10*Δ cells expressing N196K Cox10-13Myc, N196A Cox10-13Myc, and N196D Cox10-13Myc were analyzed by BN-PAGE as described for panel A. (C) Isolated mitochondria from *cox10*Δ cells expressing WT Cox10-13Myc, H317A Cox10-13Myc, and H317A,N196K Cox10-13Myc (HA,NK-13Myc), and from *coa2*Δ cells expressing H317A Cox10-13Myc and HA,NK-13Myc were analyzed by BN-PAGE as described for panel A. (D) Purified mitochondria (500 μg protein) from endogenously tagged *COX10*-3HA cells, *COX10*-3HA cells expressing WT Cox10-13Myc or N196K Cox10-13Myc, and endogenously tagged *COX10*-13Myc cells were solubilized in IP buffer, and clarified extracts were immunoprecipitated with rabbit polyclonal anti-HA beads overnight. The fractions for each co-IP were analyzed by SDS-PAGE and immunoblotting using anti-Myc and anti-HA antibodies. Load, 2% of the soluble extract; unbound, 2% of the soluble extract after incubation with the HA-conjugated beads; wash, 50% of the last wash concentrated by trichloroacetic acid precipitation; and elution, 50% of the bead elution. IP using mouse monoclonal Myc-conjugated beads provided similar results. (E) Mitochondria (30 μg protein) purified from *coa2*Δ cells expressing either WT Cox10-13Myc or H317A Cox10-13Myc and these two plasmids expressed in *trans* with untagged N196K Cox10 were analyzed for steady-state levels of Cox10 by SDS-PAGE and immunoblotting using anti-Myc antibody and Por1 as a loading control. Similarly, mitochondria (30 μg protein) purified from *cox10*Δ cells expressing H317A Cox10-13Myc in *trans* with untagged WT Cox10 or N196K Cox10 was analyzed as described.

lacked any appreciable BN complex (Fig. 5B, lane 4), although the protein was equally present as determined by steady-state SDS-PAGE analysis. The N196A mutant, which had limited suppressor activity, formed a high-mass complex that was less abundant than the N196K mutant protein. Thus, a correlation exists between the abundance of the Cox10 complex and its suppressor activity. The N196D and N196A mutant proteins formed a high-mass complex of similar abundance when expressed in *cox10*Δ cells (Fig. 5B, lanes 7 and 8).

As mentioned, the H317A mutation in Cox10 abrogates any suppressor activity of the N196K allele. However, the inactive N196K,H317A mutant Cox10 still forms a low-abundance complex in both *coa2*Δ and *cox10*Δ cells (Fig. 5C). Thus, formation of the high-mass Cox10 complex is not dependent on a catalytically active enzyme.

The enhanced Cox10 BN complex seen in chromosomally tagged Cox10 cells expressing a low-copy-number untagged N196K Cox10 from a vector suggests that the ~370-kDa complex may be a Cox10 oligomer. Two additional studies corroborate the existence of a homo-oligomer complex. First, cells expressing chromosomally HA-tagged Cox10 and vector Myc-tagged Cox10 were tested for co-IP (Fig. 5D). Precipitation of HA-Cox10 resulted in co-IP of a fraction of Myc-Cox10, especially in the cells with the N196K Cox10. Second, coexpression of the unstable H317A Cox10 mutant (Fig. 4C) with the N196K mutant led to a pronounced stabilization of the unstable H317A Cox10 in either *coa2*Δ or *cox10*Δ cells (Fig. 5E). The cotransformants of both strains were fully competent in growth on glycerol/lactate medium (data not shown). The stabilized H317A Cox10 did not have any dominant negative effects.

We sought to assess whether other components were present in the high-mass Cox10 complex by taking a candidate protein approach. Three candidates are Coa2, Cox15, and Cox1. No stable interaction between Coa2 and Cox10 was observed in co-IP studies. Cox10 functions in heme *a* biosynthesis together with Cox15. Since bacterial Cox10 and Cox15 orthologs were reported to associate within a complex (6), we tested whether

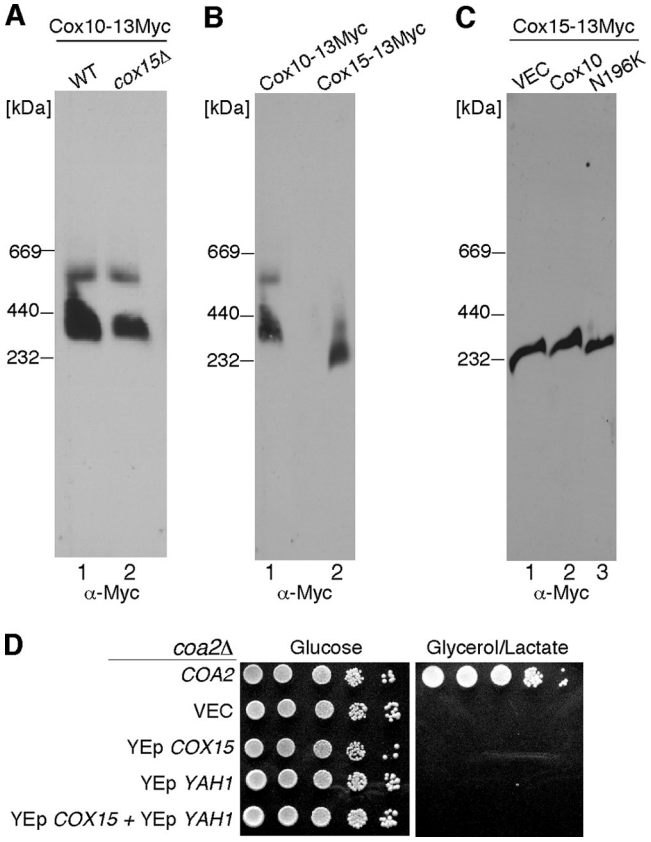

FIG. 6. Cox10 and Cox15 form distinct high-molecular-weight complexes. (A) Mitochondria (100 μg protein) isolated from WT or *cox15*Δ cells containing an endogenously tagged 13-Myc *COX10* gene were solubilized in buffer containing 1.5% digitonin. The lysates were run on a continuous 5 to 13% gradient gel, and protein complexes were separated by BN-PAGE. The Cox10-13Myc complex was detected by immunoblotting with anti-Myc antibody. Molecular mass markers are indicated. (B) Purified mitochondria from cells containing either a genomically tagged 13-Myc *COX10* gene or 13-Myc *COX15* gene were solubilized (100 μg and 30 μg mitochondrial protein, respectively) and analyzed by BN-PAGE as described for panel A. (C) Mitochondria (35 μg protein) isolated from strains containing a genomically tagged 13-Myc *COX15* gene expressing either WT Cox10 or Cox10-N196K were solubilized and analyzed by BN-PAGE as described for panel A. The Cox10-13Myc and Cox15-13Myc complexes were detected by immunoblotting with anti-Myc antibody. (D) *coa2*Δ cells transformed with *COA2*, YEp *COX15*, and/or YEp *YAH1* were grown in SC–2% raffinose–0.2% glucose selective medium, serially diluted, and drop tested on SC–2% glucose and SC–2% glycerol–2% lactate. Plates were at 30°C for 2 days (glucose) or 5 days (glycerol/lactate).

the Cox10 complex was abrogated in cells lacking Cox15 (Fig. 6A). *COX15* was deleted in cells chromosomally tagged at the *COX10* locus. The Cox10 BN complex persisted in *cox15*Δ cells, suggesting that Cox15 is not a stable component of the high-mass Cox10 complex. This conclusion is substantiated by the observation that Cox10 and Cox15 form distinct high-mass complexes on BN-PAGE that migrate at different sizes (Fig. 6B). The N196K Cox10 mutant had no effect on the abundance of the high-mass Cox15 BN complex (Fig. 6C), suggesting that the mutant Cox10 has a specific enhancement effect on the Cox10 BN complex.

Cells stalled in CcO biogenesis show limited levels of heme *o*. Overexpression of *COX15* along with the *YAH1* ferredoxin was shown to elevate heme *a* levels by greater than 50-fold (4). To assess whether high heme *a* levels were sufficient to suppress the respiratory deficiency of *coa2*Δ cells, mutant cells containing both genes on high-copy-number vectors were tested for growth on glycerol/lactate (Fig. 6D). Elevated levels of both proteins failed to impart respiratory growth. Thus, the robust suppressor activity of N196K Cox10 relates to a function of Cox10 in addition to its catalytic role in heme *o* formation.

The high-mass complexes of Mss51, Coa1, and Shy1 contain Cox1, so Cox1 is a third candidate component of the ~370-kDa Cox10 complex. Although no general Cox1 stabilization effect was observed with the N196K mutant Cox10, Cox10 may interact with Cox1 during the insertion of heme *a*. The lack of the high-mass Cox10 complex in *coa2*Δ cells may arise from Cox1 degradation. We tested whether the high-mass Cox10 complex was restored in *coa2*Δ cells overexpressing Mss51 to stimulate Cox1 translation. As can be seen in Fig. 7A (lane 3), elevated levels of Mss51 partially restored steady-state levels of the high-mass Cox10 BN complex. This result implies a link between Cox1 and the Cox10 complex. To test the involvement of early Cox1 assembly intermediates in the oligomeric Cox10 complex, cells containing chromosomally Myc-tagged *COX10* were used to construct deletions in *MSS51*, *COX14*, *COA1*, *SHY1*, or *SCO1*. The Cox10 BN complex was abrogated in all mutant strains other than *sco1*Δ cells (Fig. 7B). Cells lacking Mss51 fail to translate full-length Cox1, but cells lacking either Cox14 or Coa1 synthesize Cox1; however, the protein is unstable (28). The oligomeric Cox10 complex is largely attenuated in *cox1*Δ cells, but a residual complex persists. To assess whether the oligomeric complex of N196K mutant Cox10 is dependent on Cox1, WT and mutant Cox10 were expressed in cells lacking Mss51, Cox14, or Coa1 (Fig. 7C). Whereas neither form of Cox10 was competent to form stable oligomeric complexes in *mss51*Δ and *cox14*Δ cells, the oligomeric N196K mutant Cox10 complex was seen in *coa1*Δ cells. Levels of newly synthesized Cox1 are comparable in *cox14*Δ and *coa1*Δ cells, yet Cox10 is responsive to Cox1 levels only in *coa1*Δ cells. No direct stable interaction of Cox10 and Cox1 is observed. HA-tagged Cox1 did not co-IP with Myc-tagged Cox10 (Fig. 7D), and two-dimensional BN-PAGE failed to show comigration of Cox10 and Cox1 (data not shown). Although a co-IP of Cox10 and Cox1 was not observed, we did reproduce the known interactions of Coa1 with Cox1 and of Shyl with Cox1 (data not shown). Thus, formation of the high-mass Cox10 complex is linked to Cox1 translation and formation of the Mss51/Cox14-containing Cox1 complex, although no direct interaction between Cox10 and Cox1 exists that is stable to co-IP.

An unbiased proteomic approach was taken to identify components in the high-mass Cox10 BN complex. Digitonin-solubilized mitochondrial supernatant isolated from chromosomally tagged Cox10 cells was used for immunoprecipitation (IP) by anti-Myc agarose beads. Resolution of the IP on SDS-PAGE followed by mass spectrometry of the silver-stained bands revealed Cox10 and prohibitin subunits (Phb1 and Phb2) and the mAAA subunits (Yta10 and Yta12). Cox1 was not observed. The prohibitin and mAAA components are apparently nonspecific IP products, as prohibitin subunits also were recovered with control beads and mAAA associates with the prohibitin complex (33).

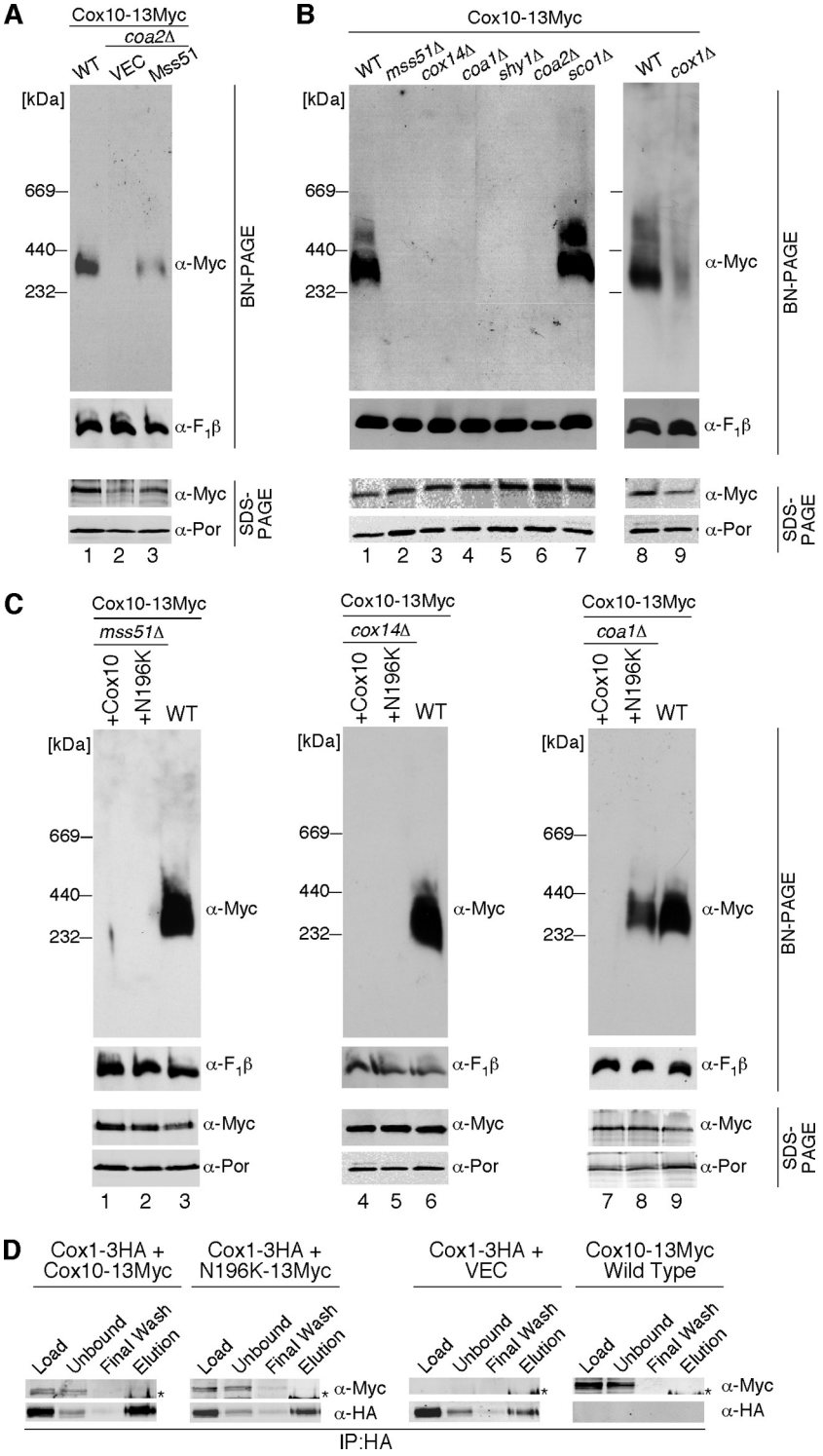

FIG. 7. Cox1 is not a stable component of the Cox10 high-molecular-weight complex. (A) Isolated mitochondria (100 μg protein) from WT, *coa2*Δ, and *coa2*Δ cells expressing YEp *MSS51* containing an endogenously tagged 13-Myc *COX10* gene were solubilized and analyzed by BN-PAGE as described previously. Detection of the $F_1\beta$ subunit of monomeric complex V was used as a loading control. The lower panel represents purified mitochondria (30 μg protein) from the same strains analyzed under denaturing (SDS-PAGE) conditions. Anti-Myc antibody was used to detect Cox10-13Myc, and Por1 was used as a loading control. (B) Mitochondria purified from WT, *mss51*Δ, *cox14*Δ, *coa1*Δ, *shy1*Δ, *coa2*Δ, *sco1*Δ, and *cox1*Δ strains containing chromosomally tagged *COX10*-13Myc were analyzed by both native (BN, 100 μg mitochondrial protein) and denaturing (SDS, 30 μg mitochondrial protein) PAGE using anti-Myc antibody. (C) Mitochondria (100 μg protein) from chromosomally tagged *COX10*-13Myc strains with *mss51*Δ (lanes 1 and 2), *cox14*Δ (lanes 4 and 5), or *coa1*Δ (lanes 7 and 8) expressing WT Cox10 or mutant N196K Cox10 were analyzed by BN-PAGE and SDS-PAGE as described previously. (D) Cox1 and Cox10 do not have a stable interaction. Mitochondria (350 μg protein) from *COX1*-3HA cells, *COX1*-3HA cells expressing YCp WT Cox10, or Cox10-N196K and *COX10*-13Myc cells were solubilized in IP buffer, and clarified extracts were immunoprecipitated with rabbit polyclonal anti-HA beads. All co-IP samples were analyzed by SDS-PAGE and immunoblotting as indicated. Details are as described for Fig. 6B. The asterisk indicates the rabbit immunoglobulin G heavy chain detected with the secondary antibody used in the analysis. Similar co-IP results were obtained using mouse monoclonal Myc-conjugated beads.

Cox1 degradation in *coa2*Δ cells by the Oma1 metallopeptidase. One dramatic effect of the N196K Cox10 mutant is the abrogation of the facile degradation of Cox1 in *coa2*Δ cells. The final question addressed is whether full respiratory activity could be restored in *coa2*Δ cells if Cox1 degradation was impaired. The mAAA is the most obvious candidate IM protease, although our previous studies with *coa2*Δ cells containing a compromised mAAA protease showed only weak respiratory growth (29). Two other protease systems besides mAAA reside within the mitochondrial IM, iAAA (Yme1) and Oma1 (Fig. 8D). The iAAA has its catalytic activity facing the intermembrane space (IMS) side of the IM and has a role in Cox2 degradation (14, 15). Oma1 is a conserved metallopeptidase that functions with the mAAA protease in the degradation of misfolded polytopic IM proteins (18). To assess whether the other IM-associated proteases contribute to the rapid Cox1 degradation seen in *coa2*Δ cells, we constructed double-deletion strains in which *OMA1* or *YME1* was disrupted in the *coa2*Δ background (Fig. 8A). The absence of Yme1 failed to markedly enhance respiratory growth of *coa2*Δ cells, but robust respiratory growth was achieved by the deletion of *OMA1*. Respiratory activity as measured by oxygen consumption was restored to ~50% of the WT level in *coa2*Δ *oma1*Δ cells (Fig. 8B), and Cox1 protein levels were restored in the *in vivo* mitochondrial translation assay (data not shown). The high-mass BN Cox10 complex was also restored in the double-null cells (Fig. 8C). Thus, respiratory function can be restored in *coa2*Δ cells either by the suppressor activity of mutant Cox10 or by selectively impaired proteolysis. A modest synergism exists between the two mechanisms. Respiratory growth of *coa2*Δ *oma1*Δ cells is enhanced by the expression of the N196K mutant Cox10 (data not shown).

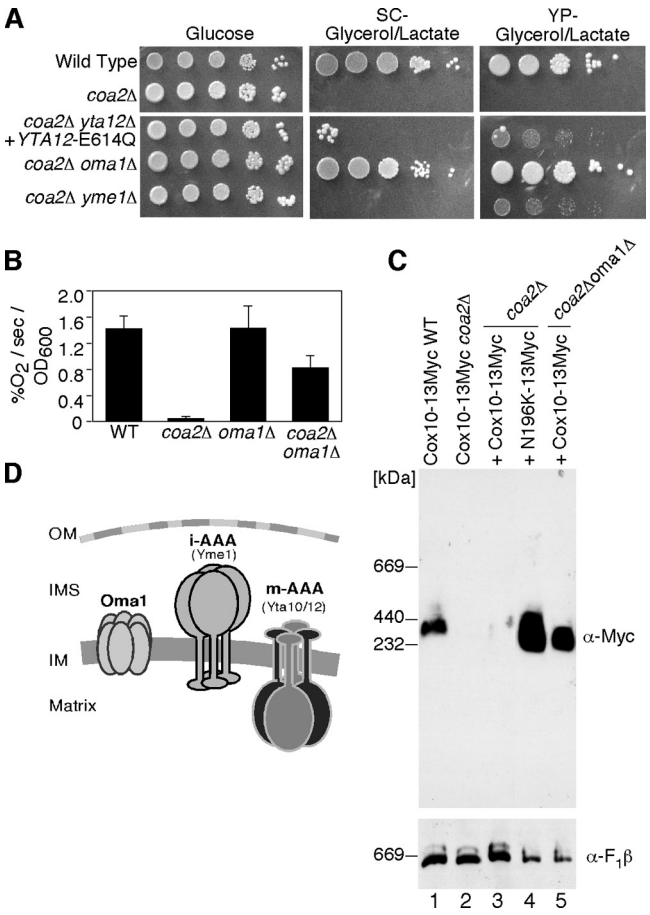

FIG. 8. Suppression of the *coa2*Δ respiratory defect by deletion of *OMA1*. (A) WT cells, *coa2*Δ cells, *coa2*Δ *yta12*Δ cells transformed with YCp Yta12(E614Q), *coa2*Δ *oma1*Δ cells, and *coa2*Δ *yme1*Δ cells were grown in SC–2% raffinose–0.2% glucose, serially diluted, and spotted onto SC–2% glucose, SC–2% glycerol–2% lactate, and yeast extract–peptone–2% glycerol-2% lactate. The plates were incubated at 30°C for 2 days (glucose) or 6 days (glycerol-lactate). (B) WT, *coa2*Δ, *oma1*Δ, and *coa2*Δ *oma1*Δ cells were grown overnight in SC–1% glucose, and oxygen consumption (% O_2/second/OD_{600} unit) was measured. The data represent the averages of three independent repeats, and the error bars represent standard errors of the means. (C) Purified mitochondria (100 μg protein) from WT or *coa2*Δ cells expressing an endogenously tagged *COX10*-13Myc, *coa2*Δ cells expressing WT Cox10-13Myc or N196K Cox10-13Myc, or *coa2*Δ *oma1*Δ cells expressing N196K Cox10-13Myc were solubilized in buffer containing 1% digitonin. Lysates were run on a continuous 5 to 13% gel, and complexes were separated by BN-PAGE. Cox10-13Myc was detected by immunoblotting with anti-Myc antisera, and monomeric complex V detected with anti-$F_1\beta$ antisera was used as a loading control. (D) A schematic of mitochondrial IM proteases. The mAAA protease is composed of Yta10 and Yta12, the iAAA protease is a homo-oligomer of Yme1, and Oma1 is proposed/speculated to be a hexamer based on previously published data (18).

DISCUSSION

Cells lacking Coa2 are stalled in CcO biogenesis and exhibit a rapid degradation of newly synthesized Cox1, leading to impaired CcO biogenesis. The respiratory deficiency of *coa2*Δ cells is suppressed either by the presence of a mutant allele of the Cox10 farnesyl transferase or by impairing proteolysis of newly synthesized Cox1 through the disruption of the Oma1 IM protease. The N196K mutant Cox10 is a gain-of-function and specific suppressor of *coa2*Δ cells. Whereas high-copy-number WT Cox10 has limited suppressor activity in restoring respiratory growth to *coa1*Δ and *shy1*Δ cells, the mutant Cox10 was no more effective than the WT protein in those CcO assembly mutants. The N196K substitution did not attenuate Cox10 catalytic activity, since the mutant protein was fully functional when expressed in *cox10*Δ cells. The mutant Cox10 restores near-WT levels of oxygen consumption in *coa2*Δ cells and Cox1 levels in the mitochondrial translation assay.

To assess the mechanism of suppression by the N196K Cox10 in *coa2*Δ cells, we showed that the mutant Cox10 lacked any general Cox1 chaperone activity. The mutant Cox10 failed to stabilize newly synthesized Cox1 in two CcO assembly mutants, *coa1*Δ and *cox4*Δ cells. The mutant and WT Cox10 were similar in having only a modest effect in enhancing the hydrogen peroxide sensitivity of *cox11*Δ cells arising from the accumulation of a prooxidant heme a_3-Cox1 assembly intermediate. If the mutant Cox10 had a general stabilizing effect on Cox1, an effect would be evident in these assays. The lack of a general stabilization effect on Cox1 was substantiated by the inability to detect any stable interaction between Cox10 and Cox1.

The suppressor function of the N196K Cox10 requires the catalytic function of Cox10. An H317A mutation that abrogates Cox10 catalysis also blocks suppressor activity of the

N196K Cox10. Likewise, the stabilization of Cox1 in the pulse phase of the mitochondrial translation assay imparted by the N196K Cox10 is dependent on a functional Cox15. Heme *a* biosynthesis is critical for the suppressor activity, although high-copy-number coexpression of Cox15 and the Yah1 ferredoxin, which is known to stimulate heme *a* formation in CcO mutants (4), lacked suppressor activity.

Cox10 forms a high-mass ~370-kDa oligomeric complex as visualized with BN gels. The abundance of the Cox10 high-mass complex seen on BN gels correlates with its suppressor activity. The complex is highly abundant in cells harboring the N196K mutant relative to the WT protein. The complex is intermediate in abundance in cells with a N196A Cox10 substitution, which has weaker suppressor activity than the N196K mutant protein. Suppressor activity and formation of the high-mass Cox10 complex are abrogated with an N196D substitution. Formation of the high-mass Cox10 complex is not dependent on a catalytically active enzyme as shown with the N196K,H317A mutant Cox10. Whereas the N196K Cox10 mutant has a marked effect on the abundance of the Cox10 BN complex, the mutant protein has no effect on the abundance of the high-mass Cox1-containing Coa1 or Shy1 complexes. Thus, the effect of the N196K mutant is restricted to the Cox10 complex.

Heme *a* biosynthesis involves both Cox10 and Cox15. Cox15 is present at nearly 10-fold-higher levels than Cox10 in yeast (37). Therefore, Cox10 may be the limiting factor in generation of heme *a*. We postulate that Cox10 has a key role in Cox1 hemylation besides its catalytic role in forming heme *o*. Cox10 appears to sense newly synthesized Cox1, although Cox10 does not stably interact with Cox1. Formation of the Cox10 oligomeric complex is dependent on Cox1 at an early step in Cox1 maturation. Cells lacking Cox14 fail to form the high-mass Mss51/Cox14-containing Cox1 complex (3, 30) and are unable to form the Cox10 oligomeric complex despite having WT levels of newly synthesized Cox1. In contrast, cells lacking Coa1 retain a WT Mss51/Cox14 complex and show an oligomeric Cox10 complex with the N196K mutant Cox10 but not the WT protein. Thus, formation of the oligomeric Cox10 complex with the WT protein appears to be dependent on the Coa1-containing Cox1 complex, but the mutant protein can oligomerize in the absence of Coa1. Coa1 may have a role in promoting Cox10 oligomer formation. An attractive postulate is that the Cox10 catalytic function is dependent on oligomerization, such that Cox10 activity is attenuated in cells lacking Coa1 or the upstream Mss51/Cox14 factors. Previously it was reported that heme *o* formation was dependent on the presence of Cox15 (4), although the mechanism by which Cox15 modulates Cox10 remains unknown. Formation of the potentially deleterious heme *a* moiety may be temporally coordinated with formation of a Cox1 assembly intermediate. This may be one mechanism to minimize the deleterious effects of stalled Cox1 assembly intermediates. Induced heme *o* synthesis may rapidly lead to heme *a* production by the abundant Cox15 followed by heme *a* insertion into Cox1. No information exists on whether heme *a* insertion is directly facilitated by Cox15 or another protein.

The marked instability of Cox1 seen in *coa2*Δ cells may arise in part from an impaired addition of heme *a*. Cox1 spans the IM with 12 transmembrane (TM) helices organized in six successive helical pairs forming a closed bundle (34). The heme *a* farnesyl tail is packed between helices 1, 11, and 12. The axial His ligands for heme *a* ligation come from His62 in helix 2 and His378 in helix 10. Thus, heme *a* binding is expected to stabilize the Cox1 helical bundle. Impaired formation of the heme *a*-Cox1 complex would therefore be expected to destabilize Cox1, leading to rapid degradation. The N196K Cox10 may specifically overcome the impaired hemylation of Cox1 in *coa2*Δ cells, and this may explain why the mutant Cox10 has no gain-of-function activity in other CcO assembly mutants.

The N196K substitution in Cox10 has a dramatic effect on the Cox10 function. Whereas a double Arg substitution in Cox10 abrogates function, activity is restored by the addition of the N196K substitution. The two Arg residues (R212 and R216) are present in a matrix-facing loop of Cox10 between TM helices 2 and 3, and Asn196 lies at the end of TM2 near the matrix boundary. The introduced Lys in the N196K substitution may restore an important positive charge needed in catalysis. The conserved Arg residues are implicated in the binding of the pyrophosphate moiety of the farnesyl pyrophosphate substrate of the Cox10-related CyoE heme *o* synthase of *E. coli* (31). Further mechanistic details on this effect are lacking, since no structural information on Cox10 is available.

Curiously, an identical mutation corresponding to N196K was reported in human Cox10 (N204K) from two related patients with a CcO deficiency disorder (36). Lymphocytes harboring the mutant human protein showed residual CcO activity, and the mutant protein restored respiratory growth in *cox10*Δ yeast cells when overexpressed but only limited growth on glycerol medium in the absence of overexpression. In contrast to the yeast N196K Cox10, the human N204K mutant Cox10 was only a weak suppressor of *coa2*Δ cells (data not shown).

The second major mechanism of suppression of the respiratory defect in *coa2*Δ cells is through depletion of the Oma1 metallopeptidase. The depletion of Oma1 restored the WT Cox10 BN complex and restored Cox1 levels seen in the mitochondrial translation assay. Oma1 was shown to function with the mAAA protease in the degradation of a misfolded polytopic protein, Oxa1 (18). The catalytic center of Oma1 appears to reside on the matrix side of the IM, although it mediated an Oxa1 cleavage site also on the IMS side of the IM. The present work clearly documents that Oma1 has a significant role in the Cox1 instability in *coa2*Δ cells. The likely Oma1 substrate is Cox1 and not Cox10, since overexpression of *MSS51* partially restores the BN Cox10 complex in *coa2*Δ cells yet fails to promote respiratory growth. In addition, only the BN Cox10 complex is depleted in *coa2*Δ cells; steady-state Cox10 levels remain normal. Thus, the observed depletion of the high-mass Cox10 complex may arise merely from Cox1 degradation of the Coa1-containing Cox1 complex. Impaired hemylation of Cox1 may lead to a misfolded Cox1 that is an efficient substrate for Oma1. We previously demonstrated that weak respiratory growth in *coa2*Δ cells is induced in cells with an attenuated mAAA. The reported proteolytic degradation of the misfolded Oxa1 was also facilitated by a combination of Oma1 and the mAAA protease (18). Future studies will address the substrate specificity of Oma1 and whether Oma1 depletion has similar effects on other CcO assembly mutants. Oma1 is conserved in metazoans, so future studies will also

address its role in Cox1 degradation in human CcO deficiency mutants.

The two mechanisms of suppression of *coa2*Δ cells have implications for the physiological function of Coa2 in CcO biogenesis. The robust suppressor function of N196K Cox10 suggests that Coa2 functions in part in a step related to heme *a* addition to Cox1. Cells lacking Coa2 fail to form the oligomeric Cox10 complex as well as the Cox1 assembly intermediates containing Coa1 and Shy1. Coa2 may impart stability to the oligomeric Cox10 complex. It is unlikely that Coa2 imparts stability to the Coa1-containing Cox1 complex, as Coa2 and Coa1 do not interact. In contrast, Coa2 forms a transient interaction with Shy1 and may contribute to its stability (29) as well as the Cox10 complex. Shy1 stabilizes the Cox1 assembly intermediate in which the Cu_B-heme a_3 bimetallic center is formed (29). In the absence of Coa2, formation of the heme *a* and Cu_B-heme a_3 centers occurs to a limited extent, leading to low levels of the prooxidant heme a_3-Cox1 intermediate that confers weak hydrogen peroxide sensitivity. Thus, Coa2 is not essential for formation of the redox centers. Future studies will address whether Coa1 and/or Coa2 mediates Cox10 oligomerization.

A second function of Coa2 involves the apparent stabilization of Cox1 during its maturation. This may arise either from a direct effect on Cox1 or indirectly by modulating a protease such as Oma1. Newly synthesized Cox1 is less stable in *coa2*Δ cells than in *cox10*Δ cells. Although Cox1 appears to be rapidly degraded in *coa2*Δ and *cox10*Δ cells (Fig. 1F), two other studies reported the appearance of newly synthesized Cox1 in mitochondrial translation assays performed on *cox10*Δ cells (3, 25). The differences in Cox1 levels seen during the pulse phase of the translation assay in the two null strains must relate to enhanced proteolysis in *coa2*Δ cells. Coa2 may be a negative regulator of a protease such as Oma1. Future studies will directly assess the role of Coa2 in IM proteolysis.

ACKNOWLEDGMENTS

We acknowledge the assistance of Greg Keller and Talina Watts in the construction of certain yeast strains and plasmids.

This work was supported by grant ES03817 from the National Institute of Environmental Health Sciences, NIH, to D.R.W. M.B. was supported by predoctoral training grant T32 DK007115 and a University of Utah Graduate Research Fellowship.

REFERENCES

1. **Barrientos, A., K. Gouget, D. Horn, I. C. Soto, and F. Fontanesi.** 2009. Suppression mechanisms of COX assembly defects in yeast and human: insights into the COX assembly process. Biochim. Biophys. Acta **1793:**97–107.
2. **Barrientos, A., D. Korr, and A. Tzagoloff.** 2002. Shy1p is necessary for full expression of mitochondrial COX1 in the yeast model of Leigh's syndrome. EMBO J. **21:**43–52.
3. **Barrientos, A., A. Zambrano, and A. Tzagoloff.** 2004. Mss51p and Cox14p jointly regulate mitochondrial Cox1p expression in *Saccharomyces cerevisiae*. EMBO J. **23:**3472–3482.
4. **Barros, M. H., and A. Tzagoloff.** 2002. Regulation of the heme a biosynthetic pathway in *Saccharomyces cerevisiae*. FEBS Lett. **516:**119–123.
5. **Bradford, N. M.** 1976. A rapid and sensitive method for the quantitation of microgram quantities of protein utilizing the principle of protein-dye binding. Anal. Biochem. **72:**248–254.
6. **Brown, B. M., Z. Wang, K. R. Brown, J. A. Cricco, and E. L. Hegg.** 2004. Heme O synthase and heme A synthase from *Bacillus subtilis* and *Rhodobacter sphaeroides* interact in Escherichia coli. Biochemistry **43:**13541–13548.
7. **Carr, H. S., G. N. George, and D. R. Winge.** 2002. Yeast Cox11, a protein essential for cytochrome *c* oxidase assembly, is a Cu(I) binding protein. J. Biol. Chem. **277:**31237–31242.
8. **Cruciat, C. M., S. Brunner, F. Baumann, W. Neupert, and R. A. Stuart.** 2000. The cytochrome *bc*1 and cytochrome *c* oxidase complexes associate to form a single supracomplex in yeast mitochondria. J. Biol. Chem. **275:**18093–18098.
9. **Diekert, K., A. I. De Kroon, G. Kispal, and R. Lill.** 2001. Isolation and subfractionation of mitochondria from the yeast *Saccharomyces cerevisiae*. Methods Cell Biol. **65:**37–51.
10. **Fontanesi, F., C. Jin, A. Tzagoloff, and A. Barrientos.** 2008. Transcriptional activators HAP/NF-Y rescue a cytochrome *c* oxidase defect in yeast and human cells. Hum. Mol. Genet. **17:**775–788.
11. **Glerum, D. M., I. Muroff, C. Jin, and A. Tzagoloff.** 1997. *COX15* codes for a mitochondrial protein essential for the assembly of yeast cytochrome oxidase. J. Biol. Chem. **272:**19088–19094.
12. **Glerum, D. M., and A. Tzagoloff.** 1994. Isolation of a human cDNA for heme A:farnesyltransferase by functional complementation of a yeast *cox10* mutant. Proc. Natl. Acad. Sci. U.S.A. **91:**8452–8456.
13. **Glerum, D. M., and A. Tzagoloff.** 1997. Submitochondrial distributions and stabilities of subunits 4, 5, and 6 of yeast cytochrome oxidase in assembly defective mutants. FEBS Lett. **412:**410–414.
14. **Graef, M., and T. Langer.** 2006. Substrate specific consequences of central pore mutations in the i-AAA protease Yme1 on substrate engagement. J. Struct. Biol. **156:**101–108.
15. **Graef, M., G. Seewald, and T. Langer.** 2007. Substrate recognition by AAA+ ATPases: distinct substrate binding modes in ATP-dependent protease Yme1 of the mitochondrial intermembrane space. Mol. Cell. Biol. **27:**2476–2485.
16. **Hell, K., W. Neupert, and R. A. Stuart.** 2001. Oxa1p acts as a general membrane insertion machinery for proteins encoded by mitochondrial DNA. EMBO J. **20:**1281–1288.
17. **Horng, Y.-C., S. C. Leary, P. A. Cobine, F. B. J. Young, G. N. George, E. A. Shoubridge, and D. R. Winge.** 2005. Human Sco1 and Sco2 function as copper-binding proteins. J. Biol. Chem. **280:**34113–34122.
18. **Kaser, M., M. Kambacheld, B. Kisters-Woike, and T. Langer.** 2003. Oma1, a novel membrane-bound metallopeptidase in mitochondria with activities overlapping with the m-AAA protease. J. Biol. Chem. **278:**46414–46423.
19. **Khalimonchuk, O., A. Bird, and D. R. Winge.** 2007. Evidence for a prooxidant intermediate in the assembly of cytochrome oxidase. J. Biol. Chem. **282:**17442–17449.
20. **Longtine, M. S., A. McKenzie, 3rd, D. J. Demarini, N. G. Shah, A. Wach, A. Brachat, P. Philippsen, and J. R. Pringle.** 1998. Additional modules for versatile and economical PCR-based gene deletion and modification in *Saccharomyces cerevisiae*. Yeast **14:**953–961.
21. **Manthey, G. M., and J. E. McEwen.** 1995. The product of the nuclear gene *PET309* is required for translation of mature mRNA and stability or production of intron-containing RNAs derived from the mitochondrial *COX1* locus of *Saccharomyces cerevisiae*. EMBO J. **14:**4031–4043.
22. **Manthey, G. M., B. D. Przybyla-Zawislak, and J. E. McEwen.** 1998. The *Saccharomyces cerevisiae* Pet309 protein is embedded in the mitochondrial inner membrane. Eur. J. Biochem. **255:**156–161.
23. **Mick, D. U., K. Wagner, M. van der Laan, A. E. Frazier, I. Perschil, M. Pawlas, H. E. Meyer, B. Warscheid, and P. Rehling.** 2007. ShyI couples Cox1 translational regulation to cytochrome *c* oxidase assembly. EMBO J. **26:**4347–4358.
24. **Mogi, T.** 2009. Probing structure of heme A synthase from *Bacillus subtilis* by site-directed mutagenesis. J. Biochem. **145:**625–633.
25. **Nobrega, M. P., F. G. Nobrega, and A. Tzagoloff.** 1990. COX10 codes for a protein homologous to the ORF1 product of *Paracoccus denitrificans* and is required for the synthesis of yeast cytochrome oxidase. J. Biol. Chem. **265:**14220–14226.
26. **Ott, M., M. Prestele, H. Bauerschmitt, S. Funes, N. Bonnefoy, and J. M. Herrmann.** 2006. Mba1, a membrane-associated ribosome receptor in mitochondria. EMBO J. **25:**1603–1610.
27. **Perez-Martinez, X., S. A. Broadley, and T. D. Fox.** 2003. Mss51p promotes mitochondrial Cox1p synthesis and interacts with newly synthesized Cox1p. EMBO J. **22:**5951–5961.
28. **Pierrel, F., M. L. Bestwick, P. A. Cobine, O. Khalimonchuk, J. A. Cricco, and D. R. Winge.** 2007. Coa1 links the Mss51 post-translational function to Cox1 cofactor insertion in cytochrome *c* oxidase assembly. EMBO J. **26:**4335–4346.
29. **Pierrel, F., O. Khalimonchuk, P. A. Cobine, M. Bestwick, and D. R. Winge.** 2008. Coa2 is an assembly factor for yeast cytochrome *c* oxidase biogenesis facilitating the maturation of Cox1. Mol. Cell. Biol. **28:**4927–4939.
30. **Preuss, M., K. Leonhard, K. Hell, R. A. Stuart, W. Neupert, and J. M. Herrmann.** 2001. Mba1, a novel component of the mitochondrial protein export machinery of the yeast *Saccharomyces cerevisiae*. J. Cell Biol. **153:**1085–1096.
31. **Saiki, K., T. Mogi, H. Hori, M. Tsubaki, and Y. Anraku.** 1993. Identification of the functional domains in heme O synthase. Site-directed mutagenesis studies on the cyoE gene of the cytochrome bo operon in *Escherichia coli*. J. Biol. Chem. **268:**26927–26934.
32. **Siep, M., K. van Oosterum, H. Neufeglise, H. van der Spek, and L. A. Grivell.** 2000. Mss51p, a putative translational activator of cytochrome *c* oxidase

subbunit-1 (*COX1*) mRNA, is required for synthesis of Cox1p in *Saccharomyces cerevisiae*. Curr. Genet. **37:**213–220.
33. **Steglich, G., W. Neupert, and T. Langer.** 1999. Prohibitins regulate membrane protein degradation by the m-AAA protease in mitochondria. Mol. Cell. Biol. **19:**3435–3442.
34. **Tsukihara, T., H. Aoyama, E. Yamashita, T. Tomizaki, H. Yamaguchi, K. Shinzawa-Itoh, R. Hakashima, R. Yaono, and S. Yoshikawa.** 1995. Structures of metal sites of oxidized bovine heart cytochrome *c* oxidase at 2.8A. Science **269:**1069–1074.
35. **Tsukihara, T., H. Aoyama, E. Yamashita, T. Tomizaki, H. Yamaguichi, K. Shinzawa-Itoh, R. Nakashima, R. Yaono, and S. Yoshikawa.** 1996. The whole structure of the 13-subunit oxidized cytochrome *c* oxidase at 2.8 A. Science **272:**1136–1144.
36. **Valnot, I., J.-C. Von Kleist-Retzow, A. Barrientos, M. Gorbatyuk, J.-W. Taanman, B. Mehaye, P. Rustin, A. Tzagoloff, A. Munnich, and A. Rotig.** 2000. A mutation in the human heme A:farnesyltransferase gene (COX10) causes cytochrome *c* oxidase deficiency. Hum. Mol. Genet. **9:**1245–1249.
37. **Wang, Z., Y. Wang, and E. L. Hegg.** 2009. Regulation of the heme A biosynthetic pathway: differential regulation of heme A synthase and heme O synthase in *Saccharomyces cerevisiae*. J. Biol. Chem. **284:**839–847.
38. **Wittig, I., H. P. Braun, and H. Schagger.** 2006. Blue native PAGE. Nat. Protoc. **1:**418–428.